SUPPORTING MATERIAL

STED Microscopy with Optimized Labeling Density Reveals 9-fold Arrangement of a Centriole Protein

Lana Lau[1], Yin Loon Lee[2], Steffen J. Sahl[1], Tim Stearns[2], and W. E. Moerner[1]

Departments of [1]Chemistry and [2]Biology, Stanford University, Stanford, CA 94305

MATERIALS AND METHODS

Cell culture and media

IMCD3 cells were grown in DME/F12 (Invitrogen) supplemented with 10% FBS at 37°C and 5% CO_2. Mouse tracheal epithelial cell (MTEC) cultures were established as previously described (1, 2). Mice were sacrificed at 2–4 months of age, and trachea were excised, opened longitudinally to expose the lumen, and placed in 1.5 mg/ml pronase E in F12-Kaighn's media (Invitrogen) at 4°C overnight. Tracheal epithelial cells were dislodged by gentle agitation and collected in F12-Kaighn's with 10% FBS. After centrifugation, cells were treated with 0.5 mg/ml DNase I for 5 min on ice and centrifuged at 4°C for 10 min at 400 *g*. Cells were resuspended in DME/F12 with 10% FBS and plated in a tissue culture dish for 3 h at 37°C with 5% CO_2 to adhere contaminating fibroblasts. Non-adhered cells were collected, concentrated by centrifugation, resuspended in an appropriate volume of MTEC-Plus medium (as described in (1)), and seeded onto Transwell-clear permeable filter supports (Corning). The air-liquid interface was established 2 days after cells reached confluence by feeding MTECs serum-free medium (1) only in the lower chamber. Cells were cultured at 37°C with 5% CO_2, and media were replaced every 2 days. All chemicals were obtained from Sigma-Aldrich unless otherwise indicated. All MTEC media were supplemented with 100 U/ml penicillin, 100 mg/ml streptomycin, and 0.25 mg/ml Fungizone (all obtained from Invitrogen).

Immunofluorescence staining

IMCD3 cells were grown on coverslips coated with poly-L-lysine. MTEC filters were excised from their plastic supports and cut into quarters to provide multiple equivalent samples for parallel staining. Samples were washed with PBS and fixed in -20°C methanol for 10 min. After fixation, cells were washed with PBS, followed by extraction and blocking with PBS containing 3% BSA, 0.1% Triton X-100 and 0.02% sodium azide (PBS-BT). Coverslips or MTEC filters were incubated first with primary antibody against Cep164 (3) diluted in PBS-BT by 8000-fold, 2000-fold, and 100-fold for the under-labeled, ideal-labeled, and over-labeled MTEC, respectively, for 1 hour at room temperature. ATTO647N-conjugated anti-rabbit secondary IgG antibodies (Active Motif) were purified by centrifugation at 2000 *g* followed by P-30 column filtration (Bio-Rad) according to the company protocol. The purified ATTO647N-secondary antibody solution was diluted in PBS-BT to 25-50 µM and incubated at room temperature for 45 min. Samples were mounted using anti-fade mounting media containing 25% w/v glycerol, 10% w/v Mowiol 4-88 (Polysciences, Inc.), 2.5% w/v 1,4-diazobicyclo-[2.2.2]-octane (DABCO) and

0.01% w/v p-phenylenediamine (PPD) in 0.1M Tris buffer (pH6.8). PPD was added fresh to the Mowiol/DABCO mixture before use. All chemicals were from Sigma-Aldrich unless specified.

STED imaging

Images were acquired with a home-built pulsed STED microscope(4). The excitation pulse train was provided by a pulsed diode laser (70 ps pulse length, 635 nm, PDL 800-B, PicoQuant), filtered with a 640/8 excitation filter (Omega), and spatially filtered with a polarization maintaining fiber (Thorlabs). The STED pulse train was provided by a titanium-sapphire modelocked oscillator (750-780 nm, 80 MHz repetition rate, Mira 900D, Coherent) and dispersed with ~30 cm of SF2 glass and 10 cm of SF6 glass followed by 100 m of polarization maintaining optical fiber (OZ Optics) to lengthen the pulses to ~200 ps. The STED laser provided a clock which was used to trigger the excitation pulse to occur just before the STED pulse. The resulting STED pulses were long-pass filtered (730LP, Omega) and passed through a vortex phaseplate (RPC Photonics) imparting a 0-2π helical phase ramp to the wavefront to generate the doughnut mode in the sample plane. The excitation and STED beams were combined sequentially by a 2 mm thick longpass dichroic (Z635RDC, Chroma) and 5 mm thick shortpass dichroic (Z710SPRDC, Chroma) and steered into the back-port of a Nikon TE300 inverted microscope, passed through a quarter-wave plate, and focused with an oil immersion objective (Plan Fluor 100x/1.3 NA, Nikon) to provide an average power of 20-60 kW cm^{-2} and 110-140 MW cm^{-2} at the sample plane, respectively. Back propagation of the sample fluorescence was collected with the same objective and passed through the same dichroics and additional emission filters (HQ679/60M emission (Chroma), and 3^{RD}650-710 emission, Omega) to remove any residual scattered excitation or STED light. An aperture corresponding to ~40% of the magnified Airy disk of the fluorescence spot was used as the confocal pinhole before focusing the emission on a Si APD detector (SPCM-ARQH-13, Perkin Elmer). STED images were recorded by scanning the sample stage (PDQ375, Mad City Labs) under control of the Imspector program (Max Planck Institute for Biophysical Chemistry, Göttingen) with a pixel size of 20-25 nm and dwell time of 0.5 ms.

Cep164 cluster fitting

For each of the 38 or 120 centrioles of the under-labeled or ideal-labeled MTEC, respectively, a region of interest (ROI) was defined as a ~1000 nm box centered on the centriole as follows. In the under-labeled case, a collection of clusters centered within a ~1000 nm square box was identified. This box was defined to be an ROI if the clusters were discerned to be localized in an ellipse of the expected diameter of ~300-400 nm or, in the case of a box containing only 1 or 2 clusters, there were no other clusters observed within a radius of ~200 nm from these clusters in question. In the ideal-labeled case, an ROI was only defined if the clusters of the centriole of interest were completely isolated from clusters of neighboring centrioles, a necessary criterion for cluster fitting. A home-written MATLAB program was used to automate fitting of the densely arranged 130 or 1023 Cep164 clusters in the under-labeled and ideal-labeled ROIs, respectively. Within a given centriole, all clusters observed above background were identified for fitting with no underlying assumption of 9-fold symmetry as follows. The clusters were fit in order of decreasing brightness. For a given cluster, a fitbox was defined containing only the cluster and not its neighbors, fit to a general 2D Gaussian with the MATLAB function lsqnonlin, and verified by eye. The Gaussian center, amplitude, major and minor widths, and angle were

free parameters while the offset was fixed. If the fit was of acceptable quality, then the emission signal inside the box was replaced with the background level to prevent interference with fitting of the next cluster. If there was a neighboring cluster which interfered with the fitting of the first cluster, then the intensity of the neighbor was brought down to half of its level above background.

For the ~5-10% of cases of ambiguously resolved pairs of adjacent clusters, we developed a method for deciding between single-cluster and double-cluster fitting as follows: we constructed a Maximum Likelihood Estimator given a model in which a given pixel intensity derives from a single (or double) Gaussian-shaped object with Poisson noise. For the image of the cluster pair in question, the maximum likelihood estimate for data incorporating Poisson noise was obtained by minimizing the negative of the function

$$\mathrm{L}\left(\theta \mid z_1,...,z_K\right) \equiv \sum_{k=1}^{K}\left(z_k \ln \lambda_i(\theta_i) - \lambda_i(\theta_i)\right)$$

where $z_1,...,z_K$ denote the pixel intensities of the image. For the single Gaussian case (i=1), the parameter was defined by $\theta_1 = (A_1, x_1, y_1, a_1, b_1, c_1)$, mean pixel intensity by $\lambda_1(\theta_1) = DC + A_1 e^{\left(-a_1(x_k-x_1)^2+2b_1(x_k-x_1)(y_k-y_1)+c_1(y_k-y_1)^2\right)}$, and (x_k, y_k) was the coordinate of the kth pixel. For the double Gaussian case (i=2), the parameter was defined by $\theta_2 = (A_2, x_2, y_2, a_2, c_2, A_2', x_2', y_2', a_2', c_2')$ and the mean pixel intensity was defined by $\lambda_2(\theta_2) = DC + A_2 e^{\left(-a_2(x_k-x_2)^2+c_2(y_k-y_2)^2\right)} + A_2' e^{\left(-a_2'(x_k-x_2')^2+c_2'(y_k-y_2')^2\right)}$. Function minimization was performed with the MATLAB function fmincon.

To determine whether the single or double Gaussian model more appropriately described data, we used the Bayesian Information Criterion (*BIC*), which selects the model with the maximal likelihood (L) but penalizes number of parameters (k) used to fit a data set of size n. The model which minimized the *BIC* was chosen.

$$BIC = -2\ln L + k\ln(n)$$

Estimation of Cep164 ring diameter

To estimate the Cep164 ring diameter of the monociliated, under-labeled, ideal-labeled, and over-labeled MTEC samples, many of which did not yield clusters which were sufficiently resolved to be fit individually, we instead fit the collective ring as follows: the Cep164 ring diameters were determined from ellipse fitting of the thresholded STED image of each ROI. Due to the non-uniformity of Cep164 cluster brightness on the single centriole level, for each ROI, a threshold was defined to differentiate the outline of the ring from background, and an ellipse was fit to the pixels in the thresholded ring. In the case of the under-labeled MTEC, only the rings which contained 5 or 6 clusters were selected to ensure sufficient data points for fitting. The average (mean) of ellipse diameters was taken, and the ring diameter for a given sample was determined as the ensemble average (mean).

Estimation of bound antibody labels

To determine the calibration of single dye brightness, a given field of view was sequentially imaged in STED mode until most of the clusters were photobleached (~20 frames). A given cluster was fit over all frames using the fitting method described above. Cluster brightness was defined as total number of photons emitted in the fitbox with background level subtracted. Although the power used to excite the STED samples varied in the range of 12 µW to 30 µW, the fluorescence signal of ATTO647N was found to be a linear function of excitation power in this regime and thus all brightnesses are referenced to 15 µW excitation at the sample plane for consistency. Cluster brightness was computed as a function of STED frame, and single dye brightness was determined as the last step before bleaching to background level.

The distributions of cluster brightness for the under-labeled and ideal-labeled MTEC were examined. For the under-labeled case, fitting to a model of single or double Gaussians was performed and the BIC was used for model selection as described above. The single dye brightness was used for the conversion of cluster brightness to ATTO647N/cluster. For the calibration of ATTO647N per secondary (2^o) antibody, N_{647N}, absorption measurements were conducted on the purified ATTO647N-antibody solution. The ratio of $<N_{647N}>=1.5$ was determined, where $[ATTO647N] = A_{644} / \varepsilon_{644}$, $[antibody] = (A_{280} - 0.045 * A_{644}) / \varepsilon_{280}$, ε_{644} = 150,000 $M^{-1}cm^{-1}$, and ε_{280} = 203,000 $M^{-1}cm^{-1}$. As an independent determination of $[ATTO647N]/[antibody]$, epifluorescence and STED imaging was conducted on single molecules of ATTO647N-antibody embedded in PVA or Mowiol+DABCO+PPD, respectively. These single-molecule images yielded a $<N_{647N}>\approx 1$, in agreement with the bulk absorption measurements.

Modeling of Cep164 ring substructure

To evaluate whether the distribution of observed clusters per ring of the optimized-labeled MTEC was consistent with the hypothesis of 9 Cep164 clusters per ring, we assumed the following simple model: a centriole had *n* possible sites (e.g. distal appendages) for cluster observation with each site having equal observation probability, and since observation of a cluster at a given site is independent of observation at another site, the distribution of observed clusters per centriole is given by binomial statistics according to the equation

$$p(k) = \binom{n}{k} q^k (1-q)^{n-k},$$

Where *n* is the assumed number of sites per centriole, *k* is the binomial random variable, *q* is the average probability of cluster observation per appendage. In a specific measurement of a total number of centrioles *N*, N_k of the observed centrioles have *k* clusters. The average probability *q* is defined from the data as follows

$$q = \frac{clusters_{observed}}{clusters_{total}} = \frac{\sum_k^n k \bullet N_k}{n \bullet N},$$

where the observed N_k values are derived from the optimized-labeled MTEC (Fig. 4b) and $N = \sum_{k}^{n} N_k$. The distribution of expected N_k computed from the model for *p(k)* (Figure S2 a-d) should be compared to the measurements from the observed ring substructure in Figure S2e. The experimental distribution agrees almost exactly with the calculated distribution for *n*=9 and much better than with that for n=8 or the broader distributions expected for *n*=10 or *n*=11.

Cep164 Cluster Orientation

The cluster orientation was defined as the cluster angle with respect to the local tangent to the centriole ring at the cluster position (determined from "Cep164 cluster fitting"). The coordinates of all of the clusters within a given centriole were fit to an interpolated function of a general ellipse using the MATLAB function *lsqnonlin*. The cluster orientation was calculated as the counterclockwise angle of the long axis of the cluster with respect to the local centriole tangent.

SUPPORTING FIGURES

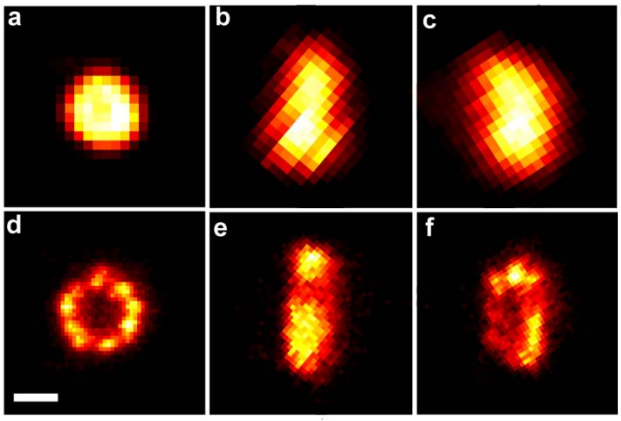

Figure S1: Cep164 ring substructure in monociliated cells. (a,b,c) Conventional diffraction-limited confocal and (d,e,f) STED images of ATTO647N immunostained Cep164 in monociliated cells taken at approximately (a,d) 0 degrees, (b,e) 90 degrees, and (c,f) an intermediate angle with respect to the ring plane. Scale bar: 200 nm.

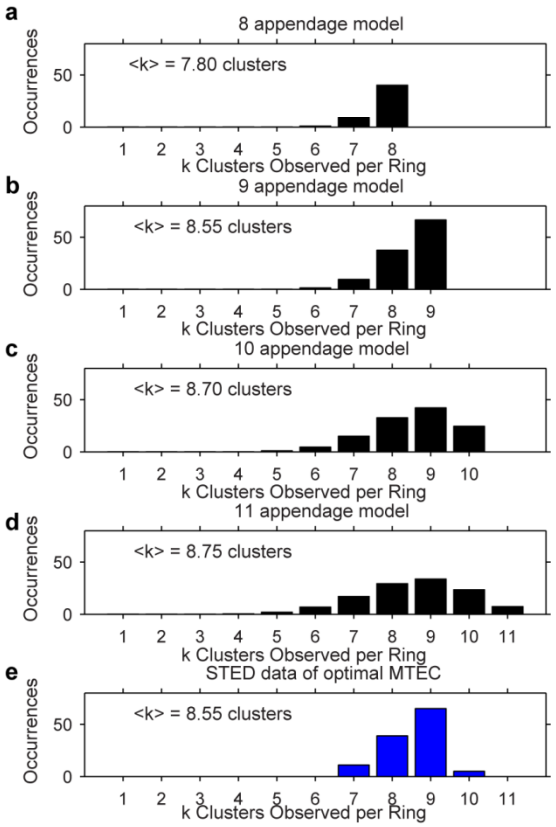

Figure S2: Modeling of Cep164 ring substructure. (a-d, black plots) Calculated binomial distribution of Cep164 ring substructure given a model of n = 8, 9, 10, or 11 appendages per centriole assuming equal probability of cluster detection per site in comparison with (e) distribution from STED measurements of optimized-labeled MTEC.

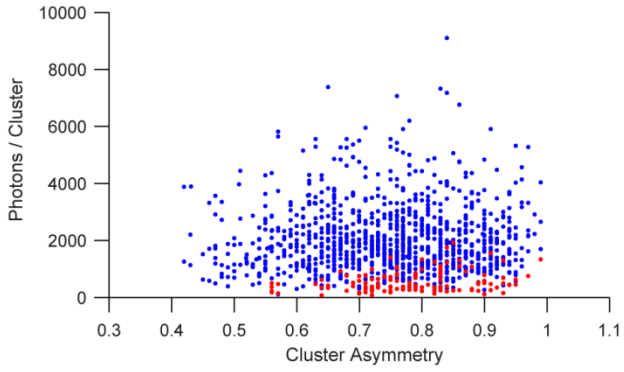

Figure S3: Correlation of cluster shape and brightness. Scatter plot of cluster asymmetry (minor diameter/major diameter) with brightness for (red) under-labeled and (blue) optimized-labeled MTEC.

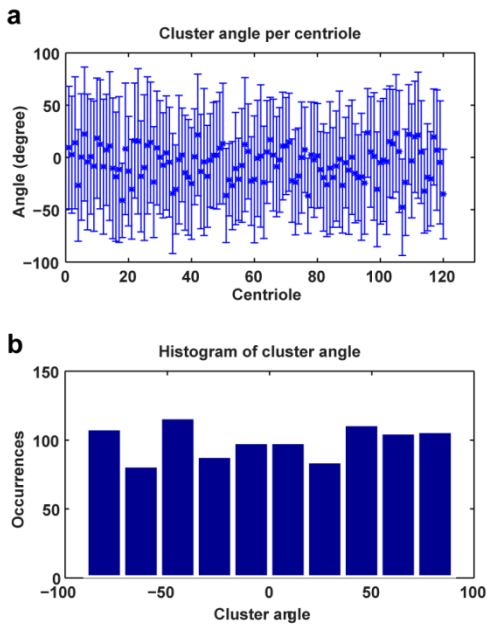

Figure S4: Cluster Orientation of Optimized-Labeled MTEC. (a) Cluster angle (angle of major axis of cluster with respect to the local centriole ring tangent) averaged per centriole and (b) individual cluster angles across all analyzed clusters for the optimized-labeled MTEC.

SUPPORTING REFERENCES

1. You, Y., E. Richer, T. Huang and S. Brody 2002. Growth and differentiation of mouse tracheal epithelial cells: Selection of a proliferative population. Am. J. Physiol. Lung Cell. Mol. Physiol., L1315.

2. Vladar, E. and T. Stearns 2007. Molecular characterization of centriole assembly in ciliated epithelial cells. J. Cell Biol. 178, 31.

3. Graser, S., Y. Stierhof, S. Lavoie, O. Gassner, S. Lamla, M. Clech and E. Nigg 2007. Cep164, a novel centriole appendage protein required for primary ciliium formation. J. Cell Biol. 179, 321.

4. Lau, L., Y.L. Lee, M. Matis, J. Axelrod, T. Stearns and W.E. Moerner 2011. STED super-resolution microscopy in *drosophila* tissue and in mammalian cells. Proc. SPIE. 7910, 79101N.